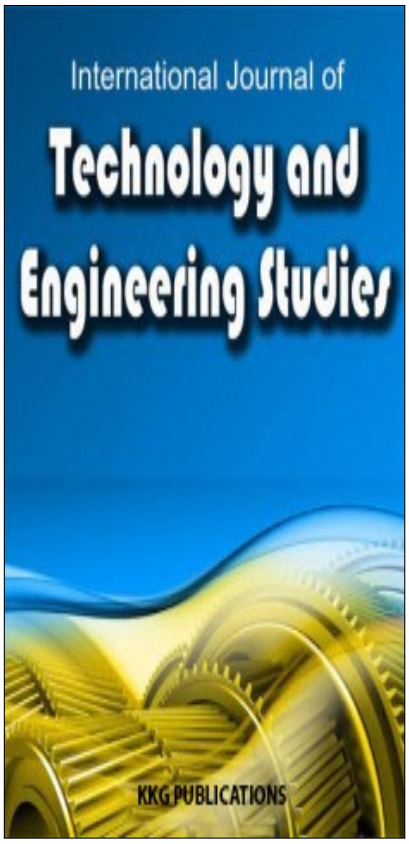

Key Knowledge Generation
Publication details, including instructions for author and subscription information:
http://kkgpublications.com/technology/

Nanoheater Underwater Robotic Welding for Marine Construction and Manufacturing

ASEEL HUSSAIN [1] , ABDELAZIZ SAEED ALZAABI [2], ABDULLA KHALED BASWAID [3], MOHAMMAD AHMAD AL MULLA [4], NOUF AL AMMARI [5], AAMNA AL JARWAN [6], SYED MURTAZA JAFFAR [7], CESARE STEFANINI [8], FEDERICO RENDA [9], CLAUS REBHOLZ [10], HARIS DOUMANIDIS [11]

[1, 2, 3, 4, 5, 6, 7, 8, 9, 11] Department of Mechanical Engineering, Khalifa University, Abu Dhabi, UAE
[10] Department of Mechanical Engineering, University of Cyprus, Nicosia, Cyprus

Published online: 24 October 2017

To cite this article: A. Hussien et al., "Nanoheater underwater robotic welding for marine construction and manufacturing," *International Journal of Technology and Engineering Studies,* vol. 3, no. 5, pp. 184-196, 2017.
DOI: https://dx.doi.org/10.20469/ijtes.3.40002-5

To link to this article: http://kkgpublications.com/wp-content/uploads/2017/3/IJTES-40002-5.pdf

International Journal of Technology and Engineering Studies
vol. 3, no. 5, pp. 184-196, 2017

IJTES

NANOHEATER UNDERWATER ROBOTIC WELDING FOR MARINE CONSTRUCTION AND MANUFACTURING

ASEEL HUSSIEN [1*], ABDELAZIZ SAEED ALZAABI [2], ABDULLA KHALED BASWAID [3], MOHAMMAD AHMAD AL MULLA [4], NOUF AL AMMARI [5], AAMNA AL JARWAN [6], SYED MURTAZA JAFFAR [7], CESARE STEFANINI [8], FEDERICO RENDA [9], CLAUS REBHOLZ [10], HARIS DOUMANIDIS [11]

[1, 2, 3, 4, 5, 6, 7, 8, 9, 11] Department of Mechanical Engineering, Khalifa University, Abu Dhabi, UAE

[10] Department of Mechanical Engineering, University of Cyprus, Nicosia, Cyprus

Keywords:
Ni/Al
Reactive Multilayers
Underwater Welding
Robot

Received: 01 January 2017
Accepted: 07 February 2017
Published: 24 October 2017

Abstract. This research introduces a 6-degree freedom underwater welding robotic system to ignite nano heater foils for metal joining, thus extending these nano heaters from soldering, brazing, and joining of components in the microchip industry to underwater welding. Ni/Al reactive multilayers are utilized to perform aluminum sheet component joining. These commercially available nano heaters release large amounts of heat when an electrical ignition stimulus initiates an exothermic reaction. The integrity of the welds performed by nano heater underwater welding is ensured by introducing openings in the nano heater foil, allowing for weld areas in a lap joint. The generated temperature field is simulated during such welding, establishing the Al sheet and nano heater thickness and the opening geometry conditions for reaching the melting temperature at the weld interface to generate successful and sound joints in the experiments. The proposed robotic system will eliminate the underwater occupational risks/hazards associated with underwater welding.

INTRODUCTION

Currently, establishing and maintaining underwater structures is hindered by several obstacles such as scarcity of highly technically skilled staff and the availability of appropriate, efficient, and safe technology, hazardous work environment [1], in addition to the economic feasibility. Underwater welding is more challenging than dry land welding due to the harsh ambient conditions such as high pressure, cooling rates, and hydrogen content [2], [3], [4], [5]. Underwater welding techniques are classified into three main categories; dry welding, wet welding, and local cavity welding [4], and [5]. In the dry welding techniques, such as dry hyperbaric welding, a chamber is evacuated from water and substituted with air or a gas mixture. On the other hand, the wet welding technique involves a professional diver carrying out welding underwater without any protection from the surrounding pressure or water. Shielded metal arc welding and flux cored arc welding are the most commonly used wet welding techniques. Wet welding allows the joining of complex underwater structures [6], [7], [8], [9], [10], [11]. However, the exposed nature of wet welding technique causes an increase in the cooling rate, which leads to the loss of ductility of weld and an increase in porosity [12], [13], [14]. Dry welding techniques produce stronger welds than wet ones, but this type of welding is more expensive since it needs extensive equipment to perform welds in dry environments. Certainly, when establishing a dry environment underwater, a wider variety of welding techniques can be utilized and stronger welds can be performed. In addition, however, dry welding takes longer time than wet welding [15], [16], [7], [17], [18]. The last underwater technique (local cavity method) offers similar conditions to open air welding. The downside of this welding mechanism is the lack of visibility. These three techniques require professional divers to perform underwater welds consequently having health risks on the divers. Previous researches aimed at understanding the relationship between such manufacturing processes and the resultant product structure and properties by inspection techniques in underwater environment, minding the interaction of the automation proximity and propulsion with the process [19], [20], [21], [22], [23], [24], [25], [26]. Researchers tried to overcome these challenges by creating automated operations to eliminate risks related to underwater manufacturing and bringing about an improved product quality, project duration, and cost through operational feasibility at higher depths [9], [19], [27], [28], [29], [30], [31], [32].

*Corresponding author: Aseel Hussien
†Email: syed.jaffar@kustar.ac.ae

This paper seeks to automate welding and inspection of aquatic infrastructures, thus enabling underwater manufacturing operations by introducing a novel and facile underwater method for both wet and dry welding based on nanoheater foils, now becoming commercially available. For the first time in the literature, this paper proposes a welding arrangement of lap metal joints with nanoheater foils at the weld interface, carrying a number of openings so that the molten metal establishes sound welding poles upon solidification without being obstructed by the refractory inter metallic products forming upon reaction of the nanoheaters. The paper also introduces an automated ignition technique of the nanoheaters by underwater robotic remotely operated vehicles without the need for welding power transmission and for precise, rigid contact of the robot with the welded structure. To the authors' knowledge, this is the first demonstration of such underwater robotic welding based on nanoheaters. Reactive multi layers are comprised of two or more energetic reactive materials placed in alternating layers. The multilayer initiate an exothermic reaction when simulated with an external stimulus [33]. There is a wide range of different reactive multilayer combinations reported in the literature. Metal/metal-oxide, metal/metal, metal/semiconductor, metal/metalloid, and metal/organic are few examples of the possible multilayers combinations. Reactive multilayer nanofoils RMNFs react either by thermal explosions or by self-propagating reactions [34]. Lately, RMNFs have attracted the attention of researchers due to their ability to join heat-sensitive components [34], [35], [36], [37]. Specifically, Ni/Al systems have small thermal penetration depths [30]. In addition, long-term storage (3 years) of Nanofoil® at room temperature caused a small increase in inter-mixing thicknesses for bilayer thicknesses greater than 35nm. This led to trivial changes inthe heat of the reaction. Consequently, it can be surmised that Nanofoils® are stable at room temperature [38]. Ni/Al multilayer systems have high heating rates, low on set reaction temperatures (below the melting point of Al and Ni), and their reaction velocity reaches 10 m/s [33]. Furthermore, they have gasless and rapid reaction rates.

Scientists are exploring other nanoheater structures; for instance, [39] proposed various methods to fabricate Ni/Al nano particles, Ni/Al nano wires, and aluminum matrix embedded with nickel particles. Galvanic replacement reaction and ultrasonic consolidation are the couple of fabrication methods used by [39].

Most researchers focused their efforts on fabricating, characterizing, and modeling the different phases of Ni/Al nano heaters in air with other combinations of nano heaters. On the other hand, this study tries to explore the feasibility of Ni/Al reactive multi layers underwater. This study aims at facilitating construction of underwater infrastructure based on welding by prefixing nano heater foils at the joints of the components. The commercially available Ni/Al RMNFs (Nanofoil®) are used to perform the welds. Ni/Al RMNFs are specifically chosen due to their attractive characteristics. These Ni/Al reactive multi layers are ignited underwater via 9V battery once the electrode is in contact with the nano foil. This instantaneous self-propagating exothermic reaction is caused by inter facial diffusion which creates low-melting phases. The reactions generate energy to overcome the heat lost to the surrounding (water) and, at the same time, melt the component surfaces all the way to the foil openings to establish the welded areas. The temperature can be increased via thermite reactions and gas blow pressure displacing water and moisture from the welding joints.

In another innovation of this paper, holes in isometric arrangement are created on the nanoheat foils to allow for flow of the component melt and strengthen the welds formed. The holes are large enough to allow maximum melt flow, while, at the same time, leaving enough Ni/Al material among the holes to reach the melting point of the component material. This optimization problem is hereby explored by finite element simulation in this research.

This paper is structured as follows: Section II describes the remotely operated underwater vehicle (ROV) used to ignite the RMNFs using attached electrodes. Section IV discusses the temperature values reached when one nanofoil is sandwiched between aluminum 6061 T6 (Al6061) plate of different thicknesses. After deducing which Al6061 plate thickness did not reach the melting point of Al6061 when using 1 Ni/Al nanofoil from section IV, the nanofoil thickness is increased to reach the liquidus melting point of Al6061 for thickness of plates. Eventually, an isometric hole array is introduced to the RMNFs to allow the flow of Al6061 melt through the holes.

REMOTELY OPERATED UNDERWATER VEHICLE (ROV)

The 6-degree of freedom underwater robotic welding system for inductive ignition by proximity to the nanoheater foil joints is also introduced and demonstrated in this study. The electrical four-thruster system uses optical video feedback and Inertial Measurement Unit (IMU) real-time control, with data transmitted to the surface on a 10 Mbps Ethernet protocol, and with a backup Li-polymer battery system on board. This tethered ROV is paired with 9V battery to perform automated underwater construction at depths up to 100 m as shown in Figure 1.

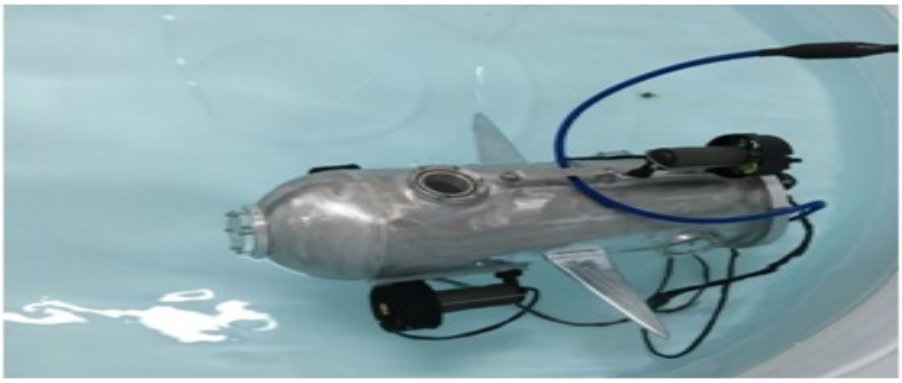

Fig. 1. ROV after assembling all thrusters, fins, end-Caps, and wiring

The ROV thrusters were designed to overcome a drag force (2.664 N) generated when it is moving at 1 knot. The thrusters are powered by commercially available sealed, brushed motors (Seabotix). The ROV uses four thrusters in total. Two Sabertooth motor controllers were utilized to control the four thrusters. Two thrusters rotating in opposite directions are used to prevent tilting (turning moment).

The ROV uses a high definition camera to help the user maneuver the ROV remotely. Sensors such as gyroscope, pressure sensor, and compass are added to the ROV to allow the user to recognize its orientation and direction. The user can control the ROV from a PC by generating commands using the live feeds of data obtained from the camera and sensors.The two electrodes are attached to 9V terminals of the battery placed inside the ROV.

One electrode is clamped to the Al6061 plate by an alligator clip or magnetic fixtures while the other electrode, which will establish contact with the nanofoil to ignite the RMNF electrically, is manipulated by the robot.

NANOFOIL IGNITION

The exothermic reaction is initiated by an electrical current provided from a 9V battery. This reaction generates a large amount of heat which melts the Al 6061 plates eventually resulting into a weld. Ignition tests are done in both ambient air and under water conditions. A 101 mm long Al6061 plate is clamped with an alligator clip attached to the positive terminal of the battery. A 0.06mm x 1.1 mm x 1.9 mm nanofoil is attached to Al6061 plate on the other end. Then a multi-wire cable as illustrated in Figure 2 connected to the negative terminal of the battery is brushed against the nanofoil which led to ignition of the nanofoil. This test setup is used for both conditions (water and air) as shown in Figure 3. The nanofoil is successfully ignited in both tests. After ignition, a NiAl phase material is produced as indicated in Figure 4.

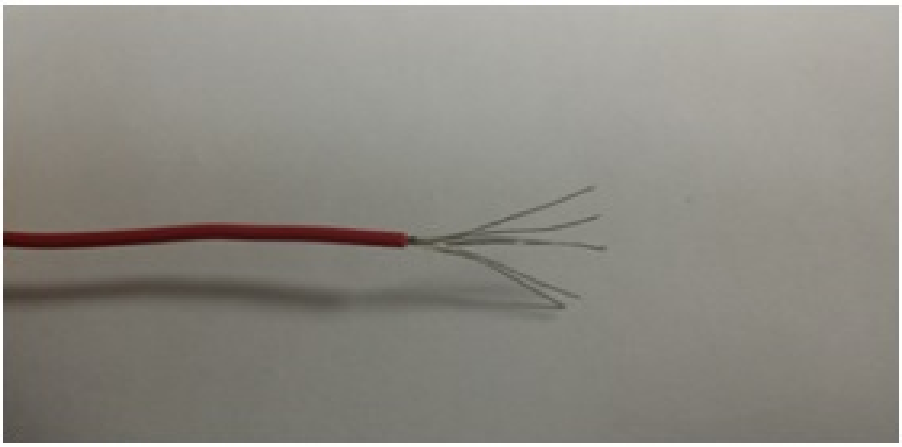

Fig. 2 Multi-wire cable

Fig. 3 The ignition test setup submerged underwater

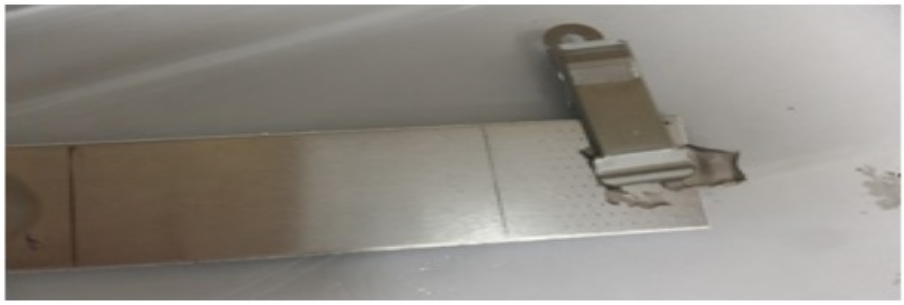

Fig. 4 Formation of NiAl after Nanofoil ignition

SIMULATIONS AND RESULTS

This section discusses the thermal simulations performed using ANSYS Workbench (Transient thermal toolbox). Initially, the temperature results of one nanofoil (h x L x L = 0.06mm x 50.8mm x 50.8mm) placed between Al6061 plates of different thicknesses are attained. Then the Ni/Al foil thickness is increased to raise the temperature values reached to ensure that the melting point of Al6061 is reached. These simulations are carried out to deduce the required nanofoil thickness to reach the melting point of the joined plates, consequently resulting into a weld. More simulations are performed on nanofoils with holes. The introduction of holes improves the strength of the welds.

Simulations Setup

ANSYS Workbench (Transient thermal toolbox) was utilized to perform the various simulations. The simulations are carried out to observe the effect of increasing plate thicknesses on the temperature response when one nanofoil is placed between the Al6061 plates. The commercially available Nanofoils of 0.06mm x 50.8mm x 50.8mm (h x L x L) dimensions are used in the simulation setup. The external faces of the sandwiched setup are perfectly insulated. A schematic illustration of the modelled system is shown in Figure 5.

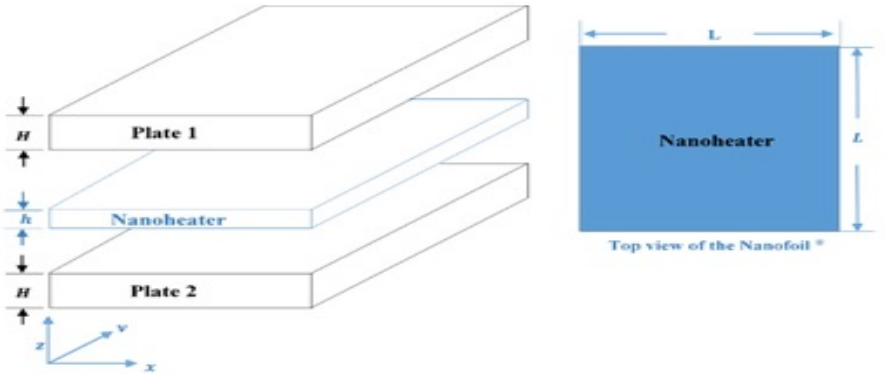

Fig. 5 Simulation model

Nanofoil properties and Aluminum 6061 properties listed in Table 1 and Table 3 respectively are assigned to the corresponding plate in ANSYS. The specific heat capacity of the Ni/Al RMNF is calculated using equation (2) using the enthalpy equation (1) and the constants summarized in Table 2.

TABLE 1
PROPERTIES OF NANOFOIL ("NANOFOIL® FOR APPLICATION", 2008)

Composition Before Reaction	Alternating Layers of Ni and Al
Composition After Reaction	$Ni_{50}Al_{50}$
Foil Density (kg/m$_3$)	5600-6000
Heat of Reaction (J/g)	1050-1250
Reaction Velocity (m/s)	6.5-8
Thermal Conductivity (W/m.K)	35-50

Assume that after the reaction, $NiAl_{(s)}$ is formed. Hence, the following equation is used to calculate the enthalpy [14].

$$\Delta H(T) = AT + \frac{B}{2}T^2 - \frac{C}{T} + \frac{D}{3}T^3 + E \tag{1}$$

$$C_p(T) = \frac{d\Delta H(T)}{dT} + BT + \frac{C}{T^2} + DT^2 \tag{2}$$

A volumetric heat generation equation is formulated to obtain the power generated by the Nanofoil per unit volume. It is assumed that a large impulse of power is generated at approximately 4.2 ms. This hypothesis is based on the following calculations. The volumetric energy released by the Nanofoil $E_{volumetric}(\frac{J}{m^3})$ is calculated as follows:

$$E_{volumetric} = Q_{average}\ x\ \rho_{average} \tag{3}$$

$Q_{average}$ is the average heat of the reaction released by Nanofoil when stimulated by external stimuli and $\rho_{average}$ is the average density of the Nanofoil specified in Table 1. The volumetric energy released per unit time provides the volumetric heat generation. The average velocity of the reaction and the width of the Nanofoil (50.8mm) are used to calculate the time as shown below:

$$D = \frac{width}{v_{average}} = \frac{L}{v_{average}} \tag{4}$$

The time taken to reach steady-state (3τ) is calculated by multiplying the time by a factor of 3. This is assumed to be the time period required to release the chemical energy of the Nanofoil.

$$3\tau = 3D \tag{5}$$

Hence, the power generated per unit volume of reactive multilayer or the volumetric heat generation $\dot{Q}$ is the volumetric energy released in 3τ.

$$\dot{Q} = \frac{E_{volumetric}}{3\tau} \tag{6}$$

The profile of the volumetric heat generation is illustrated in Figure 6. An impulse of 3.17×10^{11} watts of power is generated by $1m^3$ of Nanofoil in 4.2 milliseconds (3τ). The classical Laplace equation 7 was used to model the thermal simulations:

$$\rho C_p \frac{\partial T}{\partial t} = -k.\nabla^2 T + h \tag{7}$$

Where T is the temperature field varying with time t, and k, ρ, C_p (equations 1 and 2) are the conductivity, density, and specific heat capacity of the processed materials. As already mentioned, adiabatic boundary conditions were assumed because of the very short (few ms) duration of the nanofoil ignition leading to welding (Figure 6). The nanofoil specific volumetric heat generation $\dot{Q}$ (equations 3, 4, 5, 6) was taken from the manufacturer's specification information as above, and the material specific heat of fusion/solidification E was assumed at the melting point (660°C for Al). Both these effects are included in the enthalpic term h at the respective domains in Equation 7.

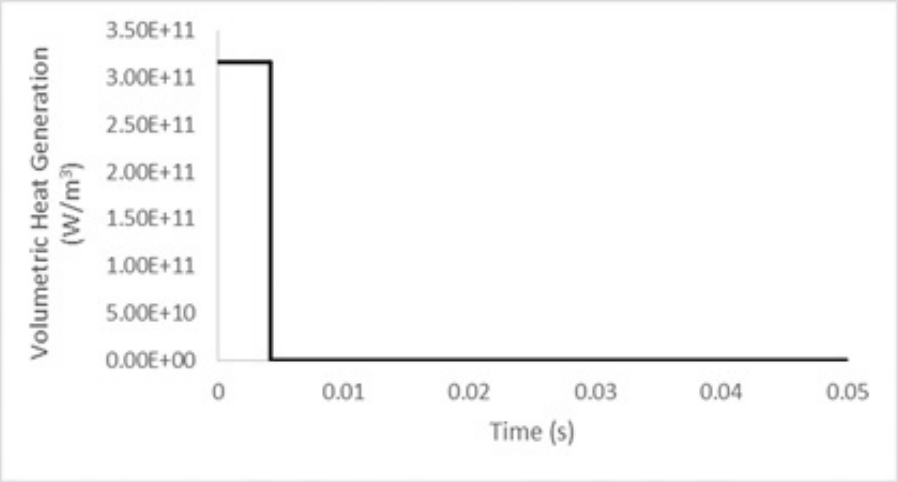

Fig. 6 The predicted volumetric heat generation profile of the Nanofoil®

Simulation Results Using One (0.06mm x 50.8mm x 50.8mm) Nanofoil® Without Holes

One nanofoil with out holes sandwiched between aluminum 6061 (Al 6061) plates of various thicknesses is simulated to approximately predict the temperature reached and confirm that the joining of the two Al 6061 is achieved. Six different simulations were performed for each Al 6061 plate thickness. The ANSYS results analyzed showed that welding occurs only when using 0.1 mm and 0.2 mm thick Al 6061 plates as shown in the Figure 7. The steady-state temperature is $T_{ss} = 1149.3$°C that is 1.8 times higher than the melting point of Al 6061 ($T_{melt} = 652$°C) when placing one 0.06mm x 50.8mm x 50.8mm between two Al 6061 plates of 0.1 mm thickness. This means that welding 0.1 mm thick Al 6061 plates is feasible using one 60μm thick Nanofoil®. Increasing the Al 6061 plate thickness to 0.2 mm led to the drop of the steady state temperature to 692°C. Hence, joining of 0.2 mm thick plates is also possible with 1 nanofoil. However, introducing holes to the nanofoil causes the energy released by the reactive multilayer to decrease, consequently lowering the steady state temperature and preventing the welding of the plates. Furthermore, simulation results indicated that the steady state temperatures significantly drop for plate thicknesses larger than 0.2 mm (i.e., 0.5 mm, 1 mm, 2 mm, and 5mm). This leads to the conclusion that thicker nanofoils are required to attain the desired steady state temperatures. By doing so, the energy released by the nanofoil increases leading to higher temperatures. Thicker nanofoils are achieved by stacking 60μm Nanofoil® on top of each other.

TABLE 2
CONSTANTS OF ENTHALPY EQUATION [19]

Phase	Temperature Range (K)	A	B x 10^3	C x 10^{-5}	D x 10^6	E x10^{-3}
NiAl(s)	298-1912	41.84	13.81	0.0	0.0	-131.5

TABLE 3
PROPERTIES OF ALUMINUM (AL 6061) [40]

Liquidus Melting Temperature (°C)	652
Density (kg/m^3)	2700
Specific Heat Capacity ($J/kg.$°C)	896
Thermal Conductivity ($W/m.$°C)	167.3

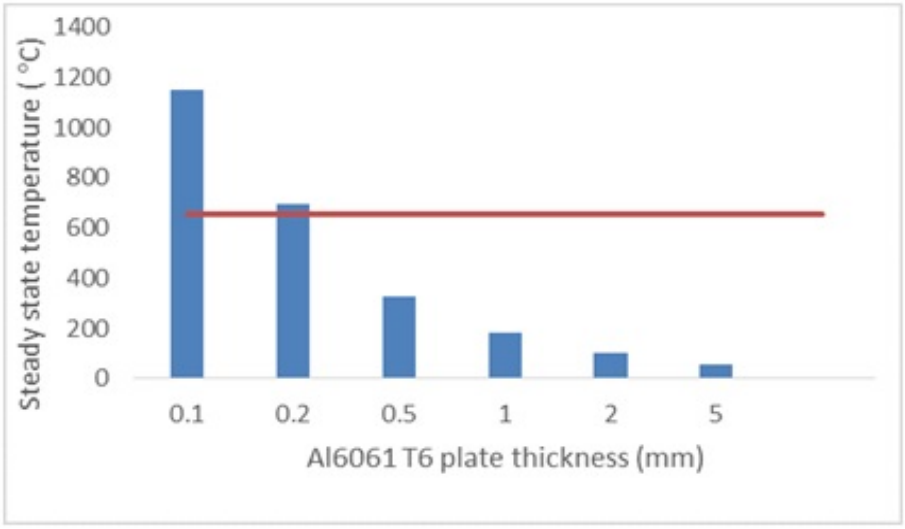

Fig. 7 Steady-state temperatures

Steady-state temperatures reached when sandwiching one 0.06mm x 50.8mm x 50.8 mm Nanofoil® between different aluminum 6061 plate thicknesses (0.1 mm, 0.2 mm, 0.5 mm, 1 mm, 2 mm, and 5 mm) compared with the liquidus melting point of Al 6061.

Simulation Results after Increasing the Thickness of Nanofoil

In this section, the Nanofoil thickness is increased (h $> 60\mu m$) to overcome the low temperature reached. The amount of reactants i.e., Ni and Al increases resulting into a higher release of energy from exothermic reaction, reaching temperatures higher than or equal to the melting point of Al 6061 which ensures welding. Multiple simulations were carried out to obtain the Nanofoil thickness needed to make welds. Table 4 summarizes the total nanofoil thickness required to achieve temperatures greater than the melting point of Al 6061.

TABLE 4
SUMMARY OF THE REQUIRED NANOFOIL THICKNESS REQUIRED TO REACH THE LIQUIDUS MELTING POINT OF AL6061 T6

Al6061 T6 Plate Thickness H-(mm)	Number of Nanofoils® (0.06mm x 50.8mm x 50.8mm)	Nanofoil® Total Thickness - h (mm)
0.1	1	0.06
0.2	2	0.12
0.5	4	0.24
1.0	6	0.36
2.0	16	0.96

Introducing Holes to the Nanofoil

Welds generated from nanofoils without holes have a layer of NiAl between the joined Al 6061 plates, which decreases the integrity of the welds. For enhancing the strength of the welds, an isometric array of holes is punched to the nanofoils as illustrated in Figure 8. Creating holes on the Nanofoil makes the welds produced stronger by allowing the flow of Al 6061 melt through the introduced holes. A total number of 22 holes are introduced to the nanofoil. Each hole is named according to its position on the nanofoil, and the letters *R* and *C* represent the row and column or location of the hole in that row, respectively. For instance, RxC 1x2 indicates the second hole inthe first row. The holes are filled with Al6061 assuming there is sufficient compressive force applied on the plates to fill the holes. A schematic illustration of the notation used to identify each hole is shown in Figure 9.

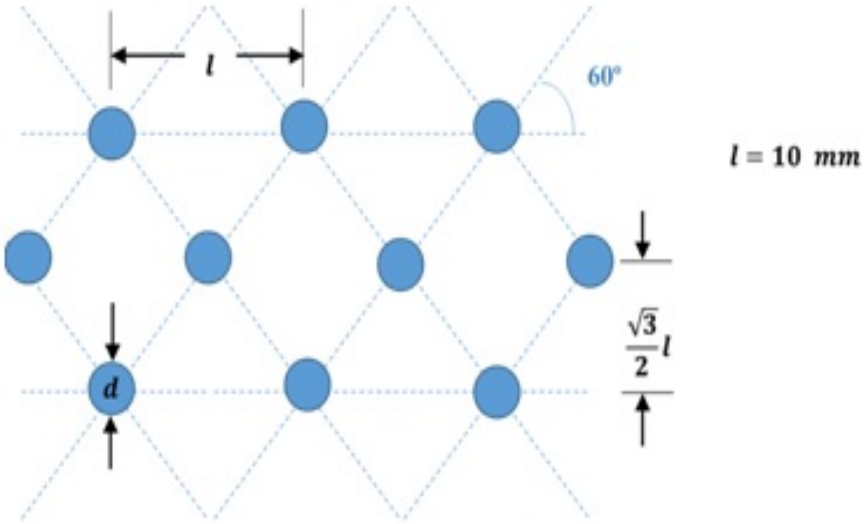

Fig. 8 Isometric hole array

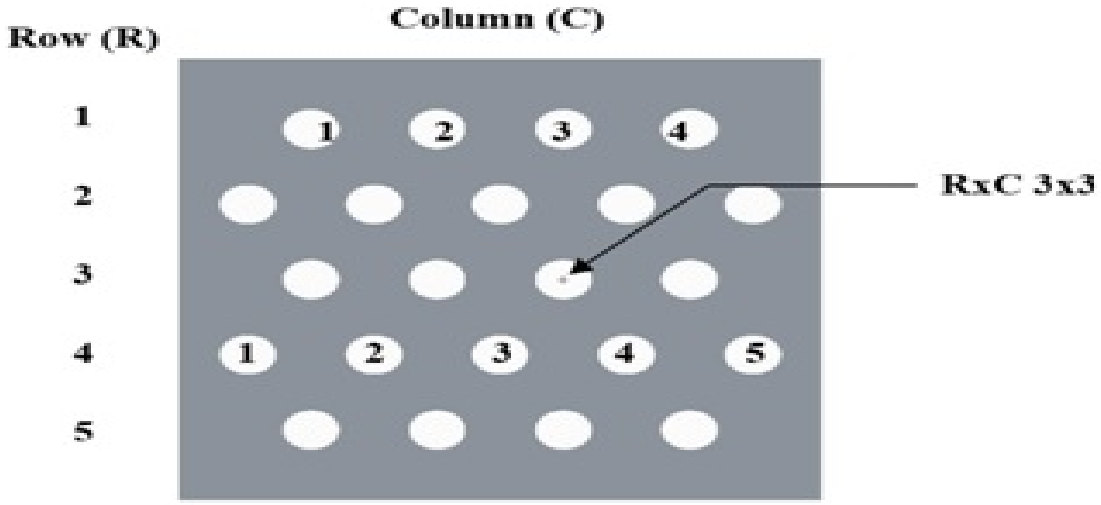

Fig. 9 The nomenclature used to indicate the holes. The temperature results considered at the center of RxC 3x3

The temperature values at the center of RxC 3x3 are specifically analyzed, since it is located at the centerline of the nanofoil. Therefore, if temperature at this point is greater than the melting point of Al 6061, it can be assumed that melting occurred at all the other holes. The temperature values versus time at the center of RxC 3x3 are analyzed. Increasing the nanofoil thickness led to a drastic rise in the temperature reached. This is evident in all the simulation results shown in Figures 10-14. This rapid rise in temperature is due to the impulse of heat generation in the first 4.2 ms as shown in Figure 6. After the instantaneous discharge of energy from the nanofoil, the temperature drops due to Newton's law of cooling. Thus, increasing the hole diameter by an increment of 0.5 mm decreases the temperature by 100°C for 0.2 mm thick Al 6061, larger holes can be introduced. It can also be observed that the temperature decreases with increasing hole diameter. This can be linked to the decrease in the amount of reactive material (Ni and Al) in the reactive multilayer. By analyzing the plots further, it can be observed that a spike in temperature (blue curves, d = 0) can be explained with the large generation of heat when the self-propagating reaction is initiated.

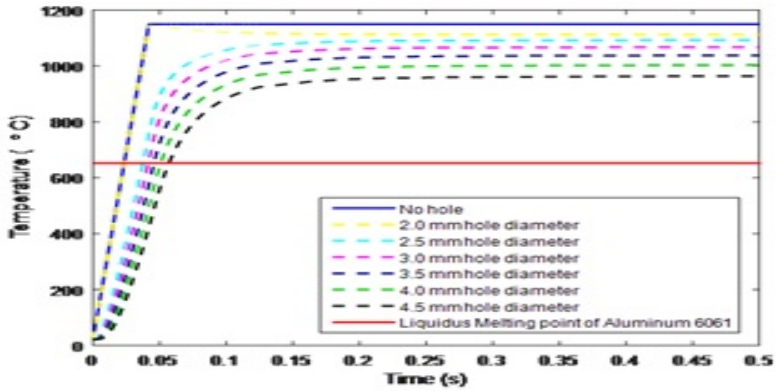

Fig. 10 Temperature response of 0.06 mm thick Nanofoil® (1 x 60 m thick foil) sandwiched between two 0.1 mm thick Aluminum plates 6061 plate. Holes of different diameters are introduced to the Nanofoils® (2.0 mm, 2.5 mm, 3.0 mm, 3.5 mm, 4.0 mm, and 4.5 mm).

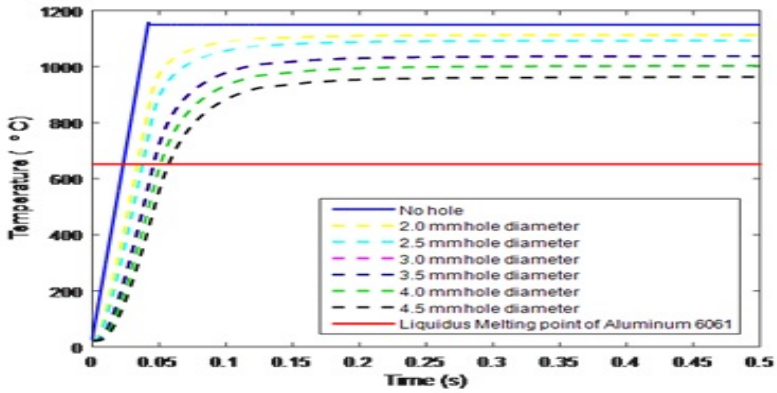

Fig. 11 Temperature response of 0.12 mm thick Nanofoil® (2 x 60 m thick foil) sandwiched between two 0.1 mm thick Aluminum plates 6061 plate. Holes of different diameters are introduced to the Nanofoils ® (2.0 mm, 2.5 mm, 3.0 mm, 3.5 mm, 4.0 mm, and 4.5 mm).

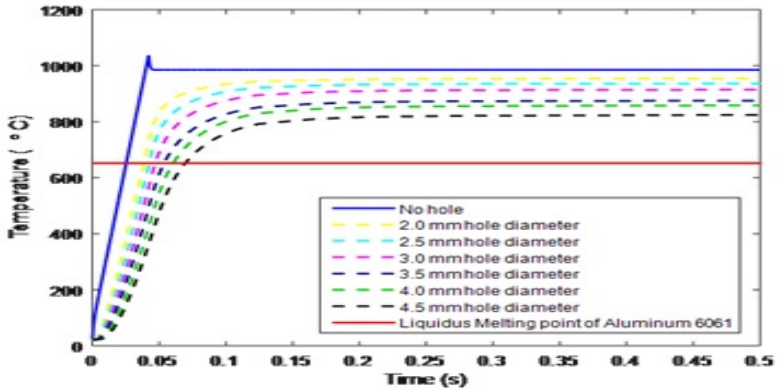

Fig. 12 Temperature response of 0.24 mm thick Nanofoil® (4 x 60 m thick foil) sandwiched between two 0.1 mm thick Aluminum plates 6061 plate. Holes of different diameters are introduced to the Nanofoils ® (2.0 mm, 2.5 mm, 3.0 mm, 3.5 mm, 4.0 mm, and 4.5 mm).

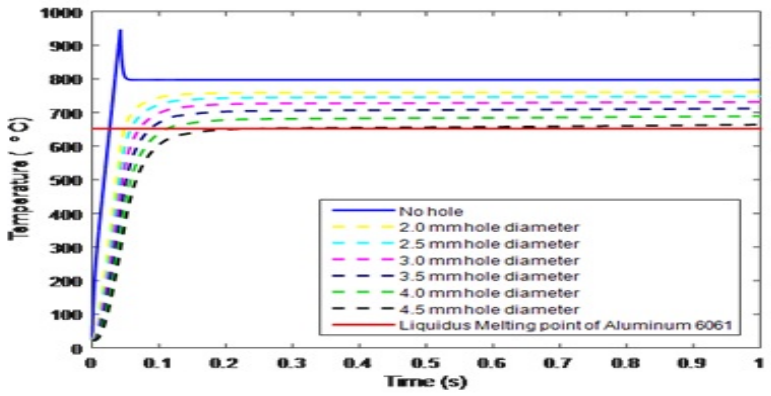

Fig. 13 Temperature response of 0.36 mm thick Nanofoil® (6 x 60 m thick foil) sandwiched between two 0.1 mm thick Aluminum plates 6061 plate. Holes of different diameters are introduced to the Nanofoils ® (2.0 mm, 2.5 mm, 3.0 mm, 3.5 mm, 4.0 mm, and 4.5 mm).

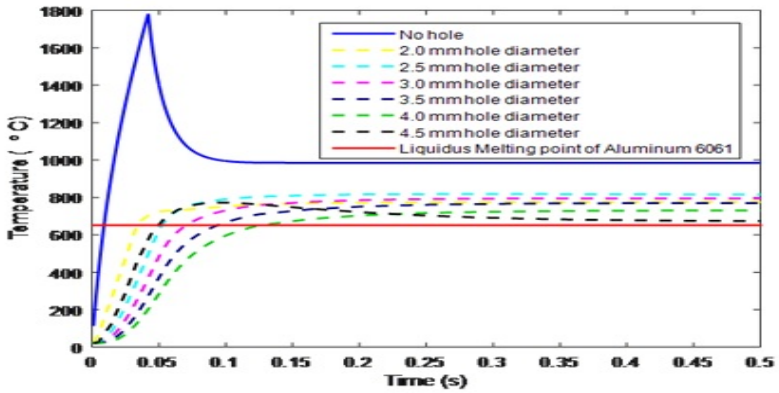

Fig. 14 Temperature response of 0.96 mm thick Nanofoil® (16 x 60 m thick foil) sandwiched between two 0.1 mm thick Aluminum plates 6061 plate. Holes of different diameters are introduced to the Nanofoils ® (2.0 mm, 2.5 mm, 3.0 mm, 3.5 mm, 4.0 mm, and 4.5 mm).

A dimensionless parameter (H/h) of the foil/nanofoil thickness ratio is derived and compared with the final temperature after 4 seconds of igniting the nanofoil. It can be noticed that as this ratio increases, the temperature reached decreases as shown in figure 15. As expected, this means thicker nanofoils (h) are required to melt thicker Al6061 plates (H).

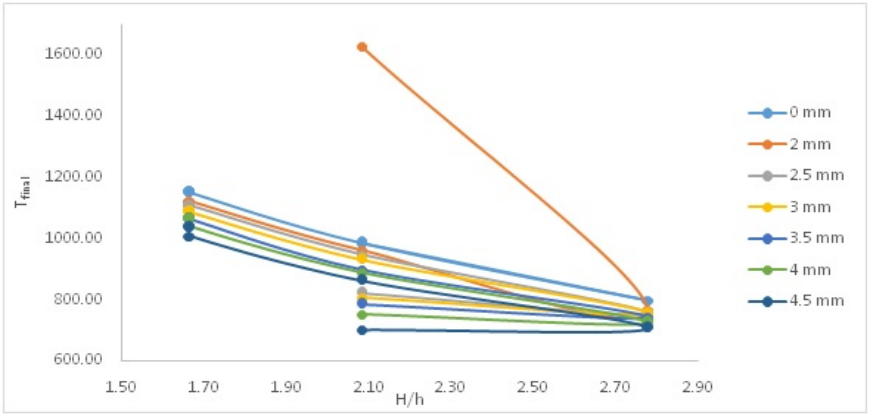

Fig. 15 Final temperature (4 seconds after igniting nanofoil) versus the dimensionless factor H/h.

CONCLUSION AND RECOMMENDATIONS

This paper has presented an automated underwater process which eliminates some of the risks accompanied with underwater welding. The use of Ni/Al reactive layers and ROV with attached electrodes have eliminated the human factor. Furthermore, the nanofoil thickness was increased to raise the steady state temperature of the system. Punching holes on the nanofoils strengthened the weld generated by allowing the flow of melted metal through the holes. Further simulations should be performed to consider the quenching effect when the joint is submerged underwater. Furthermore, Apollonian hole arrangements should be studied to see their effect on the weld strength. Future research directions also include exploring other reactive multilayer combinations such as Ru/Al systems, which generate higher temperatures and velocities. In addition, Ru/Al bimetallic foils are found to be more ductile than Ni/Al [26]. Ultrasonic consolidation might also be an interesting topic for researchers to consider in combination with nanoheater heating and leading. This technology, i.e., ultrasonically-assisted nanoheater welding, is very promising for underwater welding of metallic components. Nanofoil welding with ultrasonically-assisted techniques will offer stronger welds and might provide a simultaneous way to ignite the reactive multilayer.

Declaration of Conflicting Interests

The authors hereby declare that no conflicts of interest are present in the current study.

REFERENCES

[1] E. C. P. Pessoa, A. Q. Bracarense, E. M. Zica, S. Liu and F. Perez-Guerrero, "Porosity variation along multipass underwater wet welds and its influence on mechanical properties," *Journal of Materials Processing Technology*, vol. 179, no. 1, pp. 239-243, 2006.

[2] V. V. Chigarev and A. V. Ustinov. "Design-experimental estimation of the possibility of reduction of the HAZ metal cooling rate in wet underwater welding," *The Paton Welding Journal*, vol. 5, pp. 25-30, 2000.

[3] N. Christensen, "The Metallurgy of underwater welding," *in Internal Identity Workshop (IIW) Conference, Underwater Welding*, Pergamon Press, Trondheim, Norway, pp. 71-94, 1983.

[4] H. C. Cotton, "Welding under water and in the splash zone: A review," *in International Institute of Welding Conference*, Trondheim, Norway, pp. 63-64, June 22-23, 1983.

[5] C. Doumanidis and Y. M. Kwak, "Geometry modeling and control by infrared and laser sensing in thermal manufacturing with material deposition," *Transactions-American Society of Mechanical Engineers Journal of Manufacturing Science and Engineering*, vol. 123, no. 1, pp. 45-52, 2001.

[6] C. E. Grubbs and T. J. Reynolds, "State-of-the-art underwater wet welding," *World Oil*, vol. 219, no. 7, pp. 79-83, 1998.

[7] C. E. Grubbs and T. J. Reynolds, "Underwater welding: Seeking high quality at greater depths," *Welding Journal*, vol. 77, no. 9, pp. 35-39, 1998.

[8] S. Ibarra, C. E. Grubbs and S. Liu, "State of the art and practice of underwater wet welding of steel," in *International Workshop on Underwater Welding of Marine Structures*. New Orleans, LA, pp. 49-67, 1994.

[9] S. Liu, A. M. Pope, and R. Daemen, "Welding consumables and weldability", in *International Workshop on Underwater Welding of Marine Structures*, Lousiana, LA, pp. 321-350, 1994.

[10] V. M. Drakonakis, C. N. Velisaris, J. C. Seferis, C. C. Doumanidis, B. L. Wardle and G. C. Papanicolaou, "Matrix hybridization in the interlayer for carbon fiber reinforced composites," *Polymer Composites,* vol. 31, no. 11, pp. 1965-1976, 2010.

[11] B. R. Koh, Y. Hun Oh and D. Park, "A study on formation of saltwater-freshwater interface and upconing in coastal aquifers based on experiments with hydraulic models," *Journal of Advances in Technology and Engineering Studies*, vol. 2, no. 5, 134-139, 2016.

[12] NanoFoil® for Applications. vol. 86, no. 0, 580400, 2008.

[13] S. K. Pillai, A. Hadjiafxenti, C. C. Doumanidis, T. Ando and C. Rebholz, "Ultrasonic consolidation and ignition characteristics of thermite composites" *International Journal of Applied Ceramic Technology*, vol. 9, no. 1, pp. 206-213, 2012.

[14] S. Marchi and C. William, "Processing of aluminum-nickel intermetallics by reactive infiltration", Doctoral dissertation, Massachusetts Institute of Technology, Cambridge, MA, 1997.

[15] H. C. Cotton, "Welding under water and in the splash zone: A Review," *in International Institute of Welding Conference,* Trondheim, Norway, pp. 27-28, 1983

[16] T. G. Gooch, "Properties of underwater welds, Part 2: Mechanical properlies," *Metal Construction*, vol. 15, no. 4, pp. 164-206, 1983.

[17] J. Wang, E. Besnoin, A. Duckham , S. J. Spey, M. E. Reiss, O. M. Knio, M. Powers, M. Whitener and T. P. Weihs, "Room-temperature soldering with nanostructured foils," *Applied Physics Letters,* vol. 83, no. 19, pp. 3987-3989, 2003.

[18] K. Marat, Y. Assem, M. Bakhytzhan and K. Peter, "Theoretical and experimental researches on development of new construction of wind-driven generator with flux concentrator," *Journal of Advances in Technology and Engineering Research*, vol. 2, no. 3, pp. 100-104, 2016.

[19] M. Alaeddine, R. Ranganathan, T. Ando and C. C. Doumanidis, "Real time modeling and control in plasma arc fabrication of intermetallic coatings," in *Proceedings of the 44th IEEE Conference on Decision and Control*, Seville, Spain, pp. 3061-3066, Dec 15, 2005.

[20] H. Doumanidis and E. Skordeli, "Morphological control in desktop manufacturing by distributed attraction optimization methods," *in proceedings of the 38th IEEE Conference on Decision and Control,* Phoenix, AZ, pp. 2887-2891, December 7-10, 1999.

[21] N. Fourligkas and C. Doumanidis,"Temperature field regulation in thermal cutting for layered manufacturing," *Journal of Manufacturing Science and Engineering*, vol. 121, no. 3, pp. 440-447, 1999.

[22] P. Kamp, "Magnetic self-assembly in 3 dimensions at the macro scale," Bachelor's thesis, University of Twente, Enschede, Netherlands, 2012.

[23] V. Y. Kononenko and I. M. Savich, "Wet mechanized welding using self-shielded flux-cored wires in underwater pipes repair," in *Proceedings of the 2nd International Pipeline Technology Conference*, Ostende, Belgium, 1995.

[24] C. Rebholz, I. E. Gunduz, T. Ando and C. C. Doumanidis, "Miniature thermal matches: From nanoheaters to reactive fractals", *Materials Research Express*, vol. 2, no. 4, pp. 1-8, 2015.

[25] K. Woll, A. Bergamaschi, K. Avchachov, F. Djurabekova, S. Gier, C. Pauly, P. Leibenguth, C. Wagner, K. Nordlund and F. Mcklich. "Ru/Al multilayers integrate maximum energy density and ductility for reactive materials," *Scientific Reports,* vol. 6, pp. 1-10, 2016.

[26] P. Truttim and P. Sohsalam, "Comparison of electro coagulation using iron and aluminium electrodes for biogas production wastewater treatment," *Journal of Advances in Technology and Engineering Research,* vol. 2, no. 2, pp. 35-40.

[27] M. Calisti, M. Giorelli, G. Levy, B. Mazzolai, B. Hochner, C. Laschi and P. Dario, "An octopus-bioinspired solution to movement and manipulation for soft robots," *Bioinspiration and Biomimetics*, vol. 6, no. 3, pp. 1-6, 2011.

[28] A. Christophidou, Z. Viskadourakis and C. Doumanidis, "Structural, magnetic and dynamic mechanical analysis of magnetic nanocomposite foils by polymer ultrasonic welding," *Journal of Nano Research*, vol. 10, pp. 39-47, 2010.

[29] F. Giorgio-Serchi, A. Arienti and C. Laschi, "A soft unmanned underwater vehicle with augmented thrust capability," in *Conference of OCEANS - San Diego,* San Diego, CA, pp. 1-5, Sep 23-27, 2013.

[30] F. Renda, M. Giorelli, M. Calisti, M. Cianchetti and C. Laschi, "Dynamic model of a multibending soft robot arm driven by cables". *IEEE Transactions on Robotics*, vol. 30, no. 5, pp. 1109-1122, 2014

[31] F. Renda, F. G. Serchi, F. Boyer and C. Laschi, "Structural dynamics of a pulsed-jet propulsion system for underwater soft robots". *International Journal of Advanced Robotic Systems*, vol. 12, no. 68, pp. 1-18, 2015.

[32] M. D. Rowe, S. Liu and T. J. Reynolds, "The effect of ferro-aIloy additions and depth on the quality of underwater wet welds," *Welding Journal*, pp. 156-166, 2002.

[33] D. P. Adams, "Reactive multilayers fabricated by vapor deposition: A critical review", *Thin Solid Films*, vol. 576, pp. 98-128, 2015.

[34] B. Boettge, J. Braeuer, M. Wiemer, M. Petzold, J. Bagdahn and T. Gessner, "Fabrication and characterization of reactive nanoscale multilayer systems for low-temperature bonding in microsystem technology," *Journal of Micromechanics and Microengineering*, vol. 20, no. 6, pp. 1-8, 2010.

[35] J. Braeuer and T. Gessner, "A hermetic and room-temperature water bonding technique based on integrated reactive multilayer systems," *Journal of Micro Mechanics and Micro engineering*, vol. 24, no. 11, pp. 1-9, 2014.

[36] P. Szelagowski and I. Pachniuk, "State of the art and practice of underwater hyperbaric dry welding", in *International Workshop on Underwater Welding of Marine Structures*, New Orleans, LA, 1994.

[37] G. M. Whitesides and M. Boncheva, "Beyond molecules: Self-assembly of mesoscopic and macroscopic components", *in Proceedings of the National Academy of Sciences,* vol. 99, no. 8, pp. 4769-4774, 2002.

[38] H. Nathani, J. Wang and T. P. Weihs, "Long-term stability of nanostructured systems with negative heats of mixing," *Journal of Applied Physics*, vol. 101, no. 10, pp. 1-5, 2007.

[39] Z. Gu, Q. Cui, J. Chen, J. Buckley, T. Ando, D. Erdeniz and C. C. Doumanidis, "Fabrication, characterization and applications of novel nanoheater structures", *Journal of Surface and Coatings Technology*, vol. 215, pp. 493-502, 2013.

[40] Aerospace Specification Metals (ASM). *Properties of aluminum (AL 6061)* [online]. Available: https://goo.gl/bYns3Y

— This article does not have any appendix. —